



Controls on the development and distribution of splays in modern and ancient fluvial systems: examples from the Parapeti River, Bolivia and the Miocene Ebro basin, Spain

Linh Do Thi Thuy

PetroVietnam University, Long Toan, Ba Ria Vung Tau, Vietnam

Corresponding author: linhdt@pvu.edu.vn

ABSTRACT - The vertical and lateral aggradation of splay deposits in continental environments can form extensive sheet-like sandstones which may form an important but often overlooked component of subsurface hydrocarbon reservoirs. This study examines splay deposits of the Parapeti River, Bolivia, a modern distributive fluvial system (DFS). Overall emphasis is given to the spatial and temporal relationship between sedimentary facies at the distal part of the Parapeti River from 1972 to 2014. A sedimentary facies evolution model is created to account for the development of the distal part. Rock record examples from the Miocene Huesca DFS in the Ebro Basin (Spain) were studied in order to compare dimensional data as well as understand the relationship between splays and associated channel bodies. The study area is characterized by thin sandstone sheets interbedded with mudstones and siltstones interpreted to represent a terminal splay complex based on the distribution of facies, architectural elements and paleocurrent data. There is a strong resemblance between the model developed for the Parapeti DFS and the splay complexes recorded in the Miocene Huesca DFS. Sedimentary models are proposed in which terminal splay formation through avulsions is considered to be the dominant process in the distal parts of both systems. However, it is suggested that different types of avulsion processes recognized by previous workers, may not be distinguishable in the rock record as they can produce a similar stratigraphic signature.

Keywords: fluvial system, avulsion, splay deposits, sheet-like sandstones.

Submitted: 4 January 2021-Accepted: 25 March 2021

1. INTRODUCTION

Fine grained, sheet-like sandstone bodies deposited in continental environments form through the vertical and lateral aggradation of terminal and crevasse splay deposits. In recent years, with the increasing development of coal bed methane extraction and hydraulic fracturing of tight gas reservoirs of fluvial origin, fine-grained floodplain deposits have also been shown to be economically significant (Flores, 1985; Pashin, 1998; Ayers, 2002; Shanley et al., 2004; Scott et al., 2007; Donselaar et al., 2011). However, little, or no quantitative information on splay size, shape, connectivity, thickness, and grain size distribution is available.

In this study, geomorphological observations from the terminal area of a modern distributive fluvial system (DFS) are used to increase our understanding of how fine-grained sheet-like sandstone bodies may be developed on a modern DFS. These observations are used to develop a model for use as an analogue for better understanding

splay deposits in the rock record. The Parapeti River in the Chaco Plain, Andean Foreland Basin, South Bolivia was chosen for study, as it is an excellent example of a modern terminal fluvial systems. Results are compared with observations from splay deposits in the distal part of an ancient DFS, from the Miocene deposits of the Huesca System in the Ebro Basin (Spain) which is interpreted previously as an ancient terminal fan system (Friend, 1978; Hirst and Nichols, 1986; Hirst, 1991). From these observations a model for splay deposition and recognition in the rock record is developed.

2. THE PARAPETI RIVER

2.1. DESCRIPTION OF THE STUDY AREA

The Parapeti River is one of the largest rivers in the Chaco Plain, Andean Foreland Basin, South America (Jordan, 1995; Horton and DeCelles, 2001; Uba et al., 2006; Fig. 1). It emerges from the Andean foothills of Bolivia and flows east through San Antonio de Parapeti,

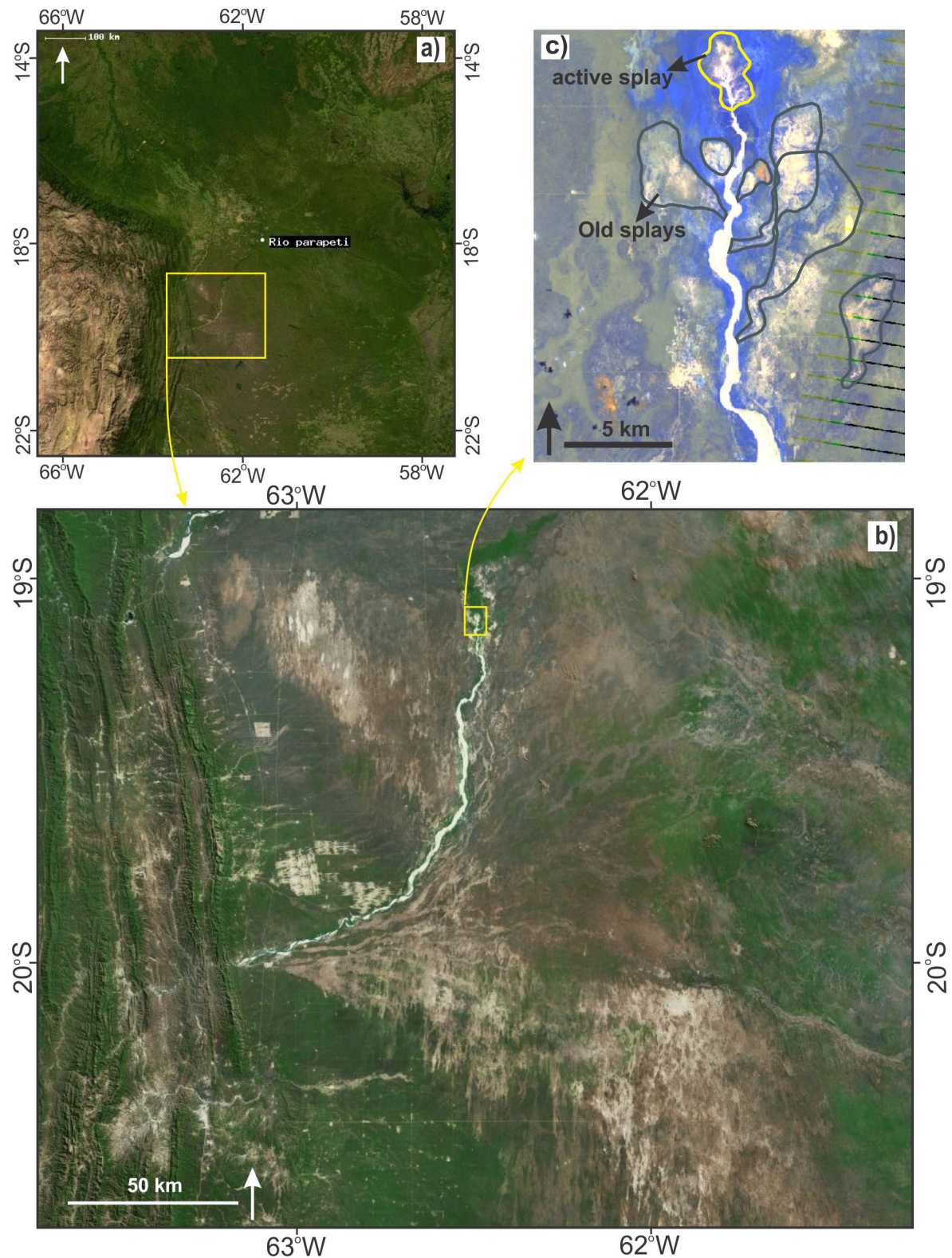


Fig. 1 - Location map of the Parapeti River. a) Locality map of Rio Parapeti; b) Location of study area (source: GoogleEarth); c) A false-color image of the river termination exhibiting splays at the distal part of the Parapeti River, the dark line indicates old splays and yellow line indicates recent splay (source: Landsat ETM+ image, <http://earthexplorer.usgs.gov>).

then northeast and turns north to terminate sub-aerially in the marshes of the Banados de Izozog, southern Bolivia (Fig. 1). The current Parapeti main channel and numerous large paleochannels form a radial, distributive

channel pattern. The fluvial megafan or DFS covers an area of at least 6,000 km² in the Chaco plain with low gradients (0.003-0.0014). The river course is around 150 km in length and characterized by a sand-bed channel.

Source-bordering transverse crescentic and parabolic dunes occur along the southern channel bank. Both active and abandoned channels generally display a downstream decrease in channel size. The active channel is up to 2.9 km in width where it exits the foothills, and narrows to 200 metres over a distance of 30 km. At the river terminus the channel width is less than 100 m from where it bifurcates into several minor distributary channels 5 to 20 m wide. Most water infiltrates or is lost through evapotranspiration, resulting in a dry channel bed during the dry season.

2.2. DATA AND METHODOLOGY

Changes in the morphology of the Parapeti River from 1972 to 2014 were investigated using Remote Sensing and Geographic Information Systems (GIS). The application of remote sensing techniques in the mapping of fluvial patterns is especially prevalent for semi-arid areas such as the Parapeti River system where using conventional ground-based investigations is particularly difficult, due to the infrequency and local nature of sediment transport events and access difficulties (Quarmby et al., 1989; Bryant, 1996). Data sets utilised here include description and interpretation of features seen in 140 carefully selected cloud-free or limited cloud cover Landsat images or image mosaics for the Parapeti fluvial system during the period 1972-2014 and CBERS (China-Brazil Earth Resources Satellite) images (Tab. 1).

Cloud-free images or those with limited cloud cover for the entire area were chosen to minimize atmospheric scatter effects, then rectified to UTM projection and the WGS 84 (World Geodetic System 1984) coordinate system. All Landsat images were preprocessed by the USGS Centre for Earth Resources Observation and Science (EROS) to correct radiometric and geometric distortions. Subsequently, image enhancement including contrast enhancement, spatial enhancement and spectral transformation was implemented in ArcMap 10 software to improve visual interpretation and understanding of

imagery. Consequently, these images were georeferenced and orthorectified into ArcGIS. Then, to achieve a broader-scale geomorphic overview, the images were visually interpreted and individual landforms were mapped. Visual interpretation incorporates colour, density and texture of the imagery, but also deduces information from elevation, vegetation and land-use patterns (Verstappen, 1977; Rosenfeld, 1984). Thus landforms, surface processes and their changes can be analysed for the investigated time period.

2.3. THE PARAPETI RIVER: MORPHOLOGICAL DEVELOPMENT

Based on the analysis of remote sensing data, a detailed inventory of geomorphological changes in the Parapeti River over the period 1972-2014 has been established. Whilst the proximal and the medial part of the river show almost no change in geomorphology and no splays were identified in these areas, the distal region of the river has experienced significant channel avulsion, terminal and crevasse splay development during the investigated period (Fig. 1c). Splays vary in scale, ranging from less than 1 km² to larger than 30 km², and distribute sediment along both banks of the river.

2.4. SPLAY TYPES

Two splay types have been identified: 1) terminal splay which migrates downstream through older splay deposits (Fig. 2) and 2) single splay which expands progressively from an initial breach point and does not migrate downstream (Fig. 3).

Type 1 or terminal splays are located on the downstream point of the river where channelized flow ceases and unchanneled floodwater spills into the wetland area (Fig. 2). Sediment is delivered onto the wetland area via distributary channels, with deposition occurring through flow expansion and a decrease in flow transport capacity (Tooth, 1999). The examples mapped are oriented parallel to the main channel with an aerial coverage ranging from

Tab. 1 - Remote sensing data sets used in the study.

Satellite	Sensor	Spatial coverage (km)	Temporal Resolution (revisit in days)	Date
Landsat 1	MSS	185 x 185	18	1972-1978
Landsat 2	MSS	185 x 185	18	1975-1982
Landsat 4	MSS	185 x 185	16	1982-1993
	TM			
Landsat 5	MSS	185 x 185	16	1984-2011
	TM			
Landsat 7	ETM+	183 x 170	16	1999-2014
CBERS 2	CCD	113 x 113	26	2004-2008
CBERS 2B	CCD	113 x 113	26	2008-2010
	HRC	27 x 27	130	2008

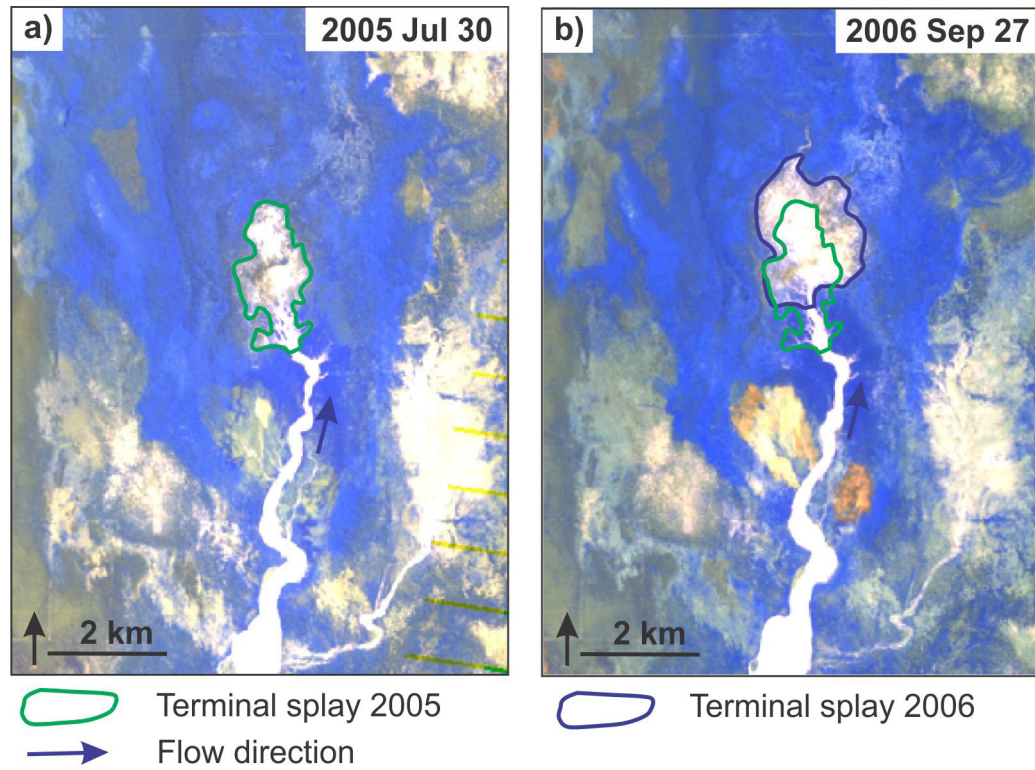


Fig. 2 - A time series of false-colour satellite images showing the development of the Parapeti terminal splay. The coloured outlines illustrate the progressive development of the terminal splay through time.

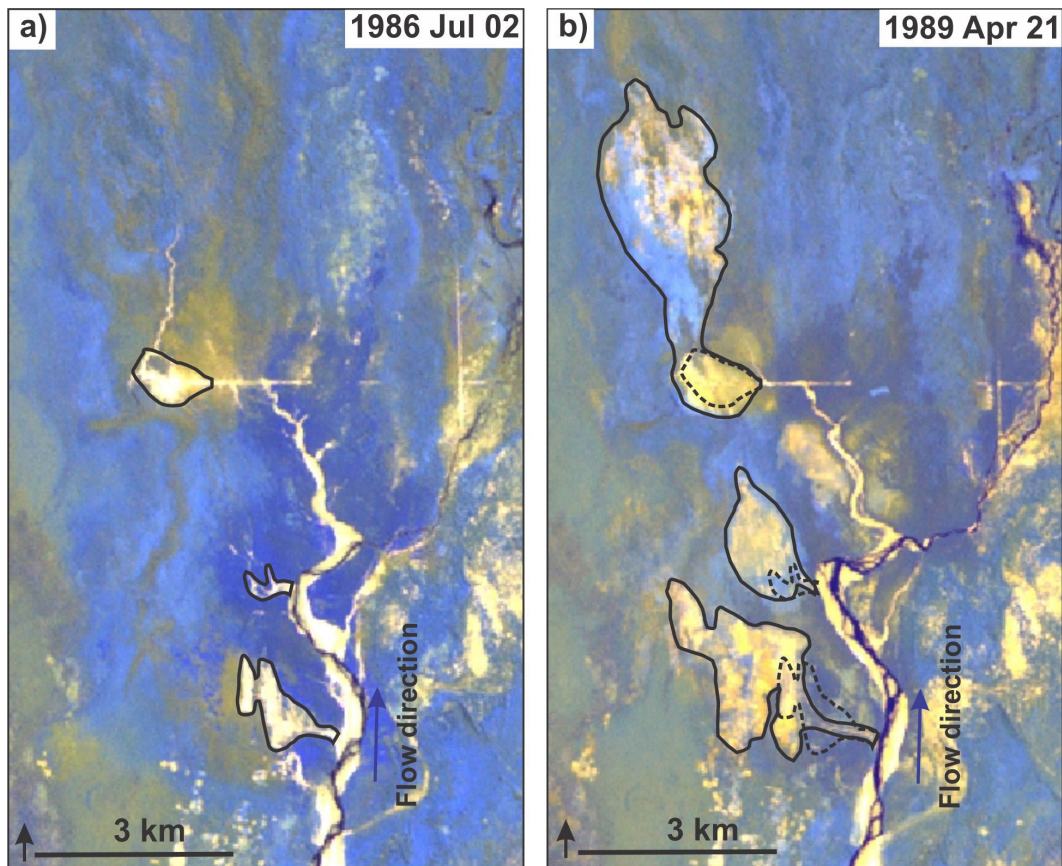


Fig. 3 - Satellite images of two different period of time showing the expansion of three splays in the distal part of the Parapeti River. Black line: boundary of splay.

0.5 to 5 km². The terminal splay illustrated in figure 2 gradually progressed through preceding splays with the terminus propagating downstream following successive flood events. Preceding splays were either degraded (through erosion associated with shallow overland flow, bioturbation or plant colonisation) or reoccupied by sediment from subsequent discharge events. This type of splay development was observed during the period 2000-2014. After 14 years, the terminal splay had migrated downstream for 6.3 km with an average progradation rate of 0.45 km per year.

Type 2 or the fixed entry splay type is a single splay that forms and expands through time but without propagation through preceding splays (Fig. 3). The initial splays have fan-like shapes, then as they develop through time, they become elongate or form an irregular pattern. This splay type has a wide range of spatial scales, from less than 1 to up to 30 km², its length ranges from several meters to 18 km. Two large splays deposits covering up to 30 km² were observed in one example. It should be noted that not every successive flow event is bigger than the previous one. Sometimes the next flow event is smaller and means that the splay size or depositional area decreases relative to earlier splays.

2.5. PARAPETI CHANNEL DEVELOPMENT

The overall development of the terminal part of the Parapeti channel is documented between 1972 and 2014, with a mix of both splay types occurring during this period. The channel prograded approximate 17 km northwards into the Izozog wetland between 1972 and 2014. Two main avulsions occurred at the river terminus between 1975 and 1984 and in 1999 (Fig. 4). These avulsions occur following a major flood event on an approximately 20-year timescale. Progradation occurs through short-term deposition in one location followed either by repeated local avulsion (Type 2) or progradation of the terminal channel and associated splay deposits coevally in a downstream direction (Type 1). It should be noted that some terminal splays appear to represent crevasse splays, as although they were originally deposited at the terminus, they have subsequently been cross-cut by the main channel during progradation of the terminal system. A simple model for the evolution of the river has been established through the analysis of Landsat time series images (Fig. 4).

In the investigated time period, the Parapeti terminal splay has migrated downstream with an average progradation rate of ~ 0.4 km per year. It should be noted that progradation did not occur every year, for example in years 2008-2009 and 2012-2014, no progradation occurred but there was still deposition during this time period and the size of the terminal splay remained similar to that of previous years.

To summarise splay development, three schematic cross-sections at different locations of the Parapeti River show the possible differences in the vertical sections of the different avulsion and splay components and are

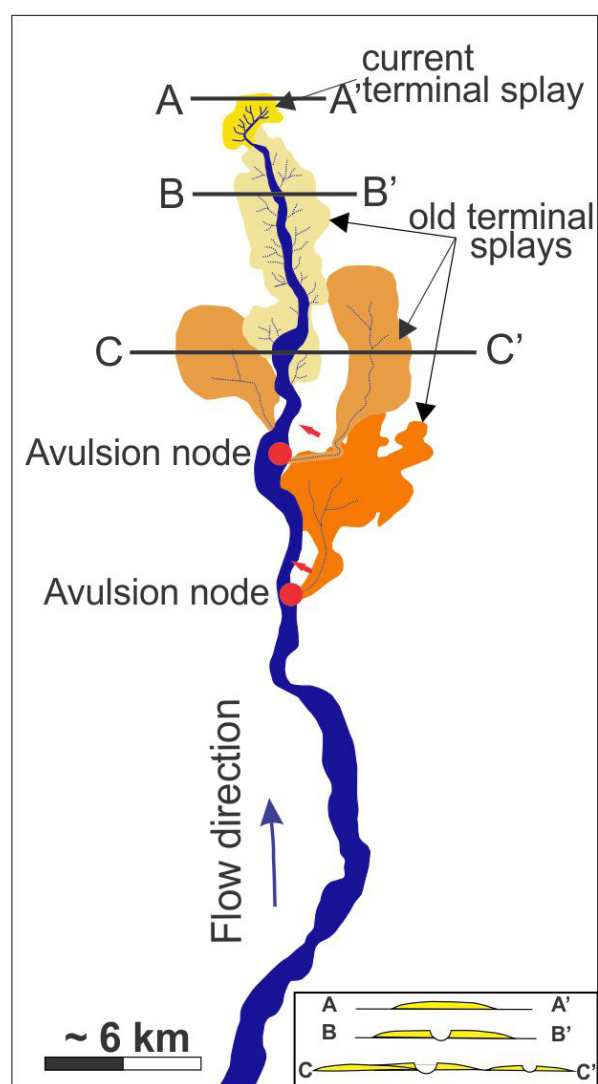


Fig. 4 - Plan and cross-section views of the terminal splays occurring in the distal sector of the Parapeti River, showing the avulsion nodes. Cross-section thicknesses are not in scale.

presented in figure 4. The sections include the current terminal splay (profile AA'), the location where the channel and the associated splays prograded coevally (profile BB') and the location where the terminal channel shifted away from the previous terminal channel position (profile CC'). The cross sectional profiles of these different avulsion and splay components are similar, except for the section across the current terminal splay which display convex-up margins without scour by channels (Fig. 4). As such, the cross-sectional profile will not be useful in determining the relative timing of splay and channel development.

3. THE HUESCA DFS SUCCESSION

3.1. DESCRIPTION OF THE STUDY AREA

The Huesca DFS is situated along the north margin of the Ebro Basin which formed as the southern foredeep of the Pyrenean orogenic belt in Miocene

times (Choukroune et al., 1989; Munoz, 1992; Teixell, 1996; Vergés et al., 2002) (Fig. 5). The fluvial sediment transported and deposited in channels and associated overbank areas of the Huesca System spread out over a fan-shaped area of >3000 km² with a radius of approximately 60 km (Hirst, 1991; Nichols and Hirst, 1998). The Huesca System deposits show radial trends in sediment texture and depositional architecture. There is an overall proximal to distal increase in the proportion of overbank deposition, while the proportion of channel deposits shows an overall reduction down-system. Grain size and sandstone-body thickness also display a general decrease down-system. Other radial trends include a change in dominant sedimentary structure from trough cross-bedding which is a prevalent feature in the medial zone, to ripple cross-lamination and concentric channel fills in the distal part (Hirst, 1991). The studied outcrop is located in the distal part of the Huesca fluvial system (Hirst and Nichols, 1986; Hirst, 1991; Fisher et al., 2007; Fisher and Nichols, 2013) and is characterized by thin sandstone sheets interbedded with mudstones, siltstones and limestones (Fig. 6).

3.2. METHODOLOGY

The investigated outcrop has a lateral extent of 750 m, and vertical thickness of 15-50 m. Detailed sedimentary logs were constructed noting bed thickness, nature of bed contacts, grain size, sorting, texture, colour, sedimentary structures, pedogenic modification, and palaeocurrent measurements (Fig. 6). These data were supported by mapping and walking out on identified key surfaces during logging and interpretation of high-resolution photo panels that have provided a physical stratigraphic framework. An east-west oriented outcrop section was chosen as it is located approximately perpendicular to the main flow direction (Hirst and Nichols, 1986; Hirst, 1991), as such, lateral as well downstream variations in the distal architectural elements could be determined.

3.3. RESULTS

Five sedimentary facies are recognised (Tab. 2) and three facies associations have been identified by grouping related sedimentary facies: 1) splay deposits, 2) splay channel, 3) floodplain (Fig. 7, Tab. 3).

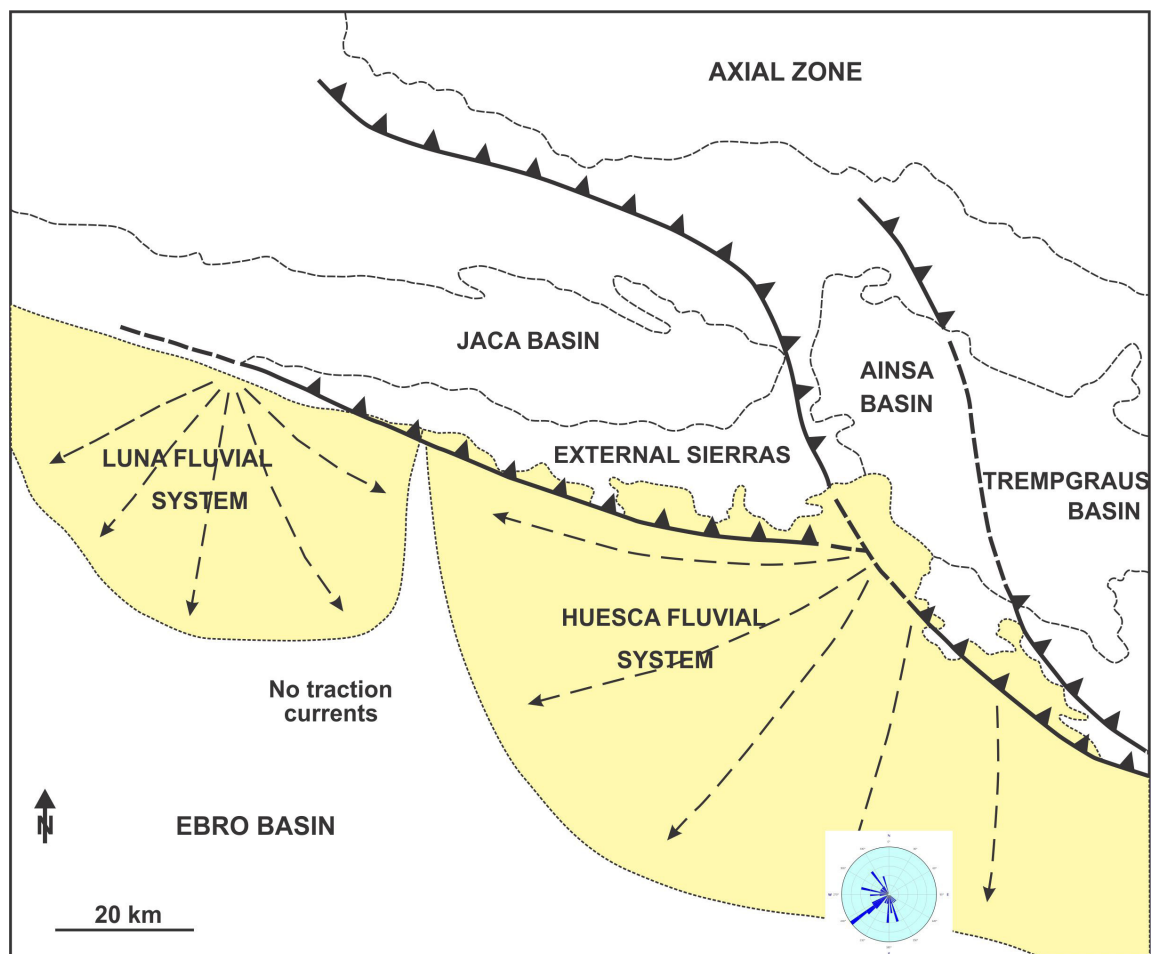


Fig. 5 - Map showing the location and terminal distributive pattern of the Luna and Huesca systems (modified from Hirst and Nichols, 1986). The position of paleocurrent diagram indicates the approximate location of the outcrop in figure 6.

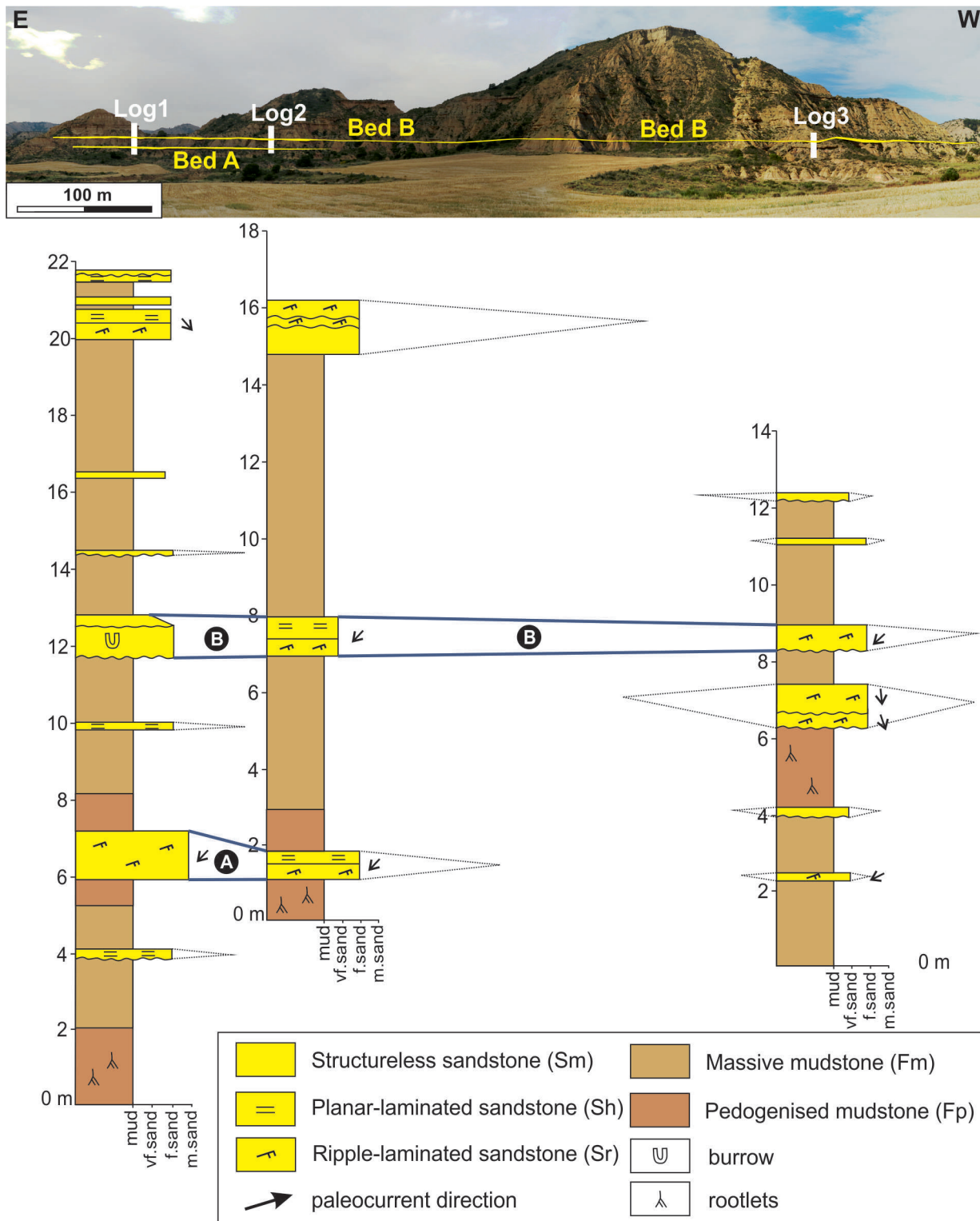
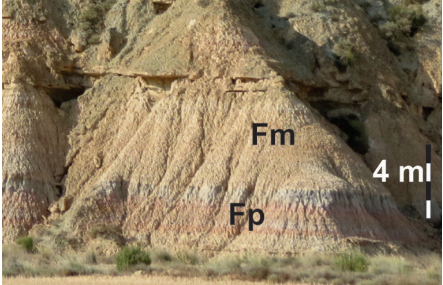
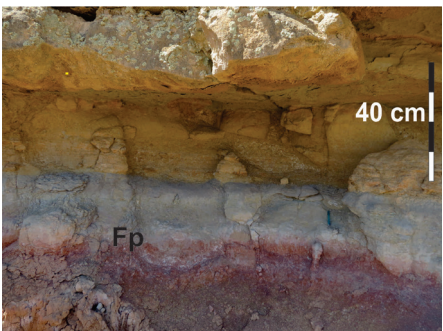


Fig. 6 - Photo panel with sedimentary log positions and detail log profiles in the study area. Dotted lines refer to the relative positions where the sandstone sheets disappear laterally. The paleocurrent direction is the mean direction measured from several measurements, however, only one measurement was recorded for the sheet sandbody at the top of log 1. A and B beds are laterally correlated with their thickness on a distance of a few hundred meters.

Splay deposits (Facies association 1-FA1): mainly comprises very fine to medium-grained sandstones. Deposits are either massive, planar-laminated or ripple cross-laminated. Individual splay deposits form laterally

extensive sheets over 100s of metres in width, a single sheet sandstone was traced for 350 m. Vertical and lateral variation in grain size within individual beds was rarely observed. Thicknesses of individual sandstone sheets

Tab. 2 - Sedimentary facies and identifying codes referred to in this study.

Facies code	Sedimentary facies	Interpretation	
Sm	Massive/structureless sandstone	Deposition by sheetflood events	
Sh	Planar-laminated sandstone	Deposition in an unconfined sheetflood setting	
Sr	Ripple-laminated sandstone	Product of waning flow	
Fm	Massive mudstone	Overbank deposition	
Fp	Pedogenised mudstone	Overbank deposition and modification by water table fluctuation	

range from 0.05 to 1.3 m, typically less than 1 m. A series of sandstone sheets and interbedded mudstone horizons stack to form deposits up to 3 m thick. The contact

between individual sandstone sheets is commonly sharp or with a slightly erosive base (~5 cm), rarely relatively erosive bases were seen (15-20 cm). Mudstone horizons

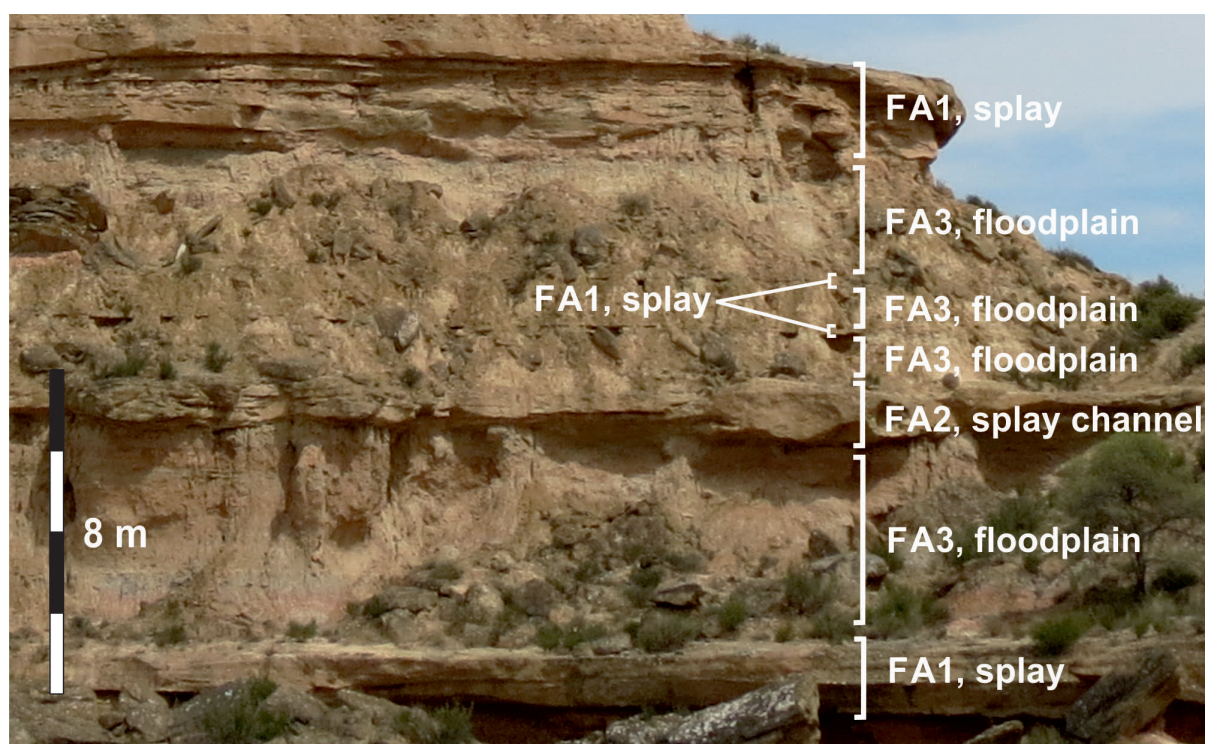


Fig. 7 - Outcrop showing the main facies associations recognized in the investigated area.

Tab. 3 - Facies associations, sedimentary facies codes and their geometry observed in the study area.

Facies associations		Sedimentary facies	Geometry
FA1	Splay deposits	Sm, Sh, Sr, Fm	Sheet sandstones
FA2	Splay channel	Sm, Sh, Sr	Ribbon sandstones
FA3	Floodplain	Fm, Fp	Laterally extensive mudstones

are generally less than 5 cm thick with a marked absence of bioturbation or paleosol development. An amalgamated package typically comprises two to three mudstone horizons separating up to six individual sandstone sheets (Fig. 7). The vertical and lateral amalgamation of individual sandstone deposits can form a sandstone package averaging 0.85 m thick and hundreds of metres wide, with several sandstone packages exceeding the width of the outcrop. These stacked sheet sandstone packages are bounded by mudstones/siltstones with flat, sharp upper contacts and sharp or gently erosional lower contacts. Occasionally, relative erosional lower contacts were observed. Convex-up mounds comprising a convex-up sandstone deposits beneath several sandstone bedsets which show an offlapping geometry over both sides of the lower sandstone unit were observed (Fig. 8). The lowest sandstone unit of this mound exhibits planar lamination, while the upper sandstone bedsets show ripple cross lamination. Both upper and lower units are fine-grained. This feature is approximately 6-7 m in length and less than 0.8 m high. The lowest convex-up sandstone unit is around 4 m in length and 0.6 m high.

The scale and sheet-like geometry of the deposits, together with the sedimentary structures are suggestive of deposition associated with poorly confined channel to unconfined flow and are interpreted as lateral or terminal splay deposits that are the result of overbank flood events. The erosively-based sandstone sheets may be interpreted as product of partly confined channel flow incising into underlying deposits. Variation in sandstone sheet dimensions suggests that they have been deposited from differing magnitude flow events. The amalgamated nature of the multiple sheets indicating multiple flow events (Fisher et al., 2007) with relatively short repeat times as indicated by the lack of bioturbation or paleosol development. The dipping bed surfaces indicate that the flows interacted with positive topographic relief developed on the floodplain, which could be related to the development of a lobe-like geomorphic feature.

Splay channel (Facies association 2-FA2): are the proximal component of splays and are closely associated with FA1. The sedimentary facies included in this facies association are massive/structureless sandstone, planar-

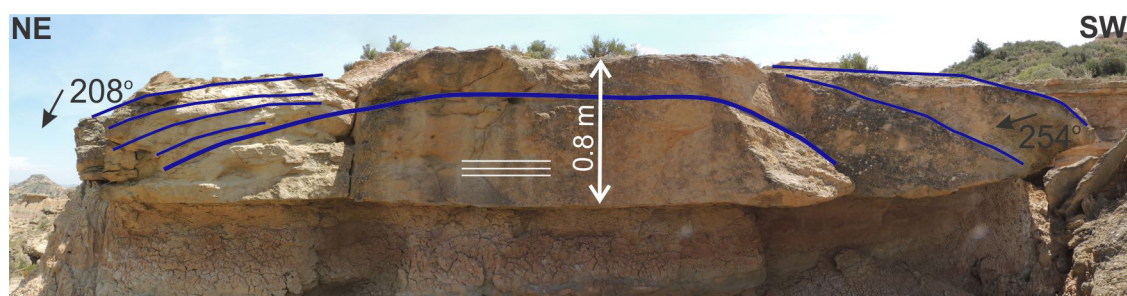


Fig. 8 - Strike-section of a fine-grained sandstone body showing the lenticular geometry of a splay, having a central sandstone unit with planar lamination and the sandy lateral accretion units which display an offlapping geometry. Blue lines indicate bed surfaces bounding sandstone units deposited during flow events.

laminated sandstone and ripple-laminated sandstone. This facies association contains ribbon deposits from terminal, lateral and crevasse feeder channels. The ribbon sandstone bodies observed in the study area consist of massive, structureless fine-grained. They are mostly less than 2 m thick and typically have an erosional contact with underlying units (mudstones and/or sandstones). In cross-section, the ribbons show thicknesses ranging from 0.5 to 1.5 m in the central, thickest part and wedge out laterally over a distance of 1.5 m to 8 m to form wings (0.05 - 0.15 m thick) that extend into adjacent mudstones/sandstones (Fig. 9). The thicknesses of sandstone bodies are generally slightly greater than the depth of the scour (0.4-1.2 m).

Small ribbon sandstones with wings intercalated with floodplain deposits are interpreted as splay channel deposits (Friend et al., 1979; Anderson, 2005). The geometry, lack of depositional structures, grain size variation and association of these ribbons with sheet sandstones and mudstones suggest that they may have been formed by choking of distributary paleo-channels due to high sediment supply at the distal part of a DFS. This occurs where terminal distributary channels cut through underlying older splays as a terminal splay progrades basinwards (Friend et al., 1986; Fisher et al., 2007). Local avulsion shifted terminal channels to new positions detaching abandoned channels from direct supply of sediment and water. Subsequently, abandoned terminal channels were filled with sand through overbank deposition from the active channel. Alternatively, the channels may be filled as result of waning flow conditions following a sheetflood event (Miall, 1996), but the lack of a fining upwards motif and the massive, structureless nature of the sandstone bodies argues against this. FA2 contains ribbon deposits from terminal, lateral and crevasse feeder channels. The differences between these deposits are only distinguished through map pattern data and paleocurrent measurements.

Floodplain (Facies association 3-FA3): comprises packages of mudstone/siltstone and pedogenically modified mudstone. The deposits are laterally extensive, often exceeding the outcrop width (~750 m) and form sheet-like bodies up to 9 m thick. Floodplain deposits

vary in colour between buff coloured, mottled red and grey. The colour changes observed have been attributed to fluctuations in the height of the groundwater table which is influenced by variable fluvial discharge. The floodplain deposits likely signify vertical accretion on alluvial plains under low energy suspension-settling conditions (Allen, 1964).

Paleocurrent Data: Overall, 48 data points were recorded within the sandstone bodies. The data show a radial dispersion with predominant paleoflow towards the south-west. The distribution of paleocurrent orientations in the rose diagram (Fig. 5) would suggest deposition in a radial, fluvial distributive system having main flow directions to the south-west. The mean vector to the south-west identified from the field area in this study is in agreement with the conclusions of the regional south-west direction of the main Huesca channel system by Hirst and Nichols (1986) and Hirst (1991).

Variations in sandstone body thickness: two specific units, labeled as Bed A and Bed B from the outcrop were traced laterally (Fig. 6).

Bed A is a single sheet sandstone, Bed B is an amalgamated sandstone sheet. Bed A with paleoflow towards the south-west indicates that the exposure is a down-current section. Overall, bed A thins down current from ~1.3 m to 0.05 m over a distance of ~350 m and shows a decrease in grain size downstream from medium to fine sandstone. This is interpreted to indicate a downstream decrease in energy which can be attributed to flow expansion. Bed B with average paleocurrents to the south-west indicates that two exposure sections are perpendicular and parallel to the main paleoflow. Generally, the thickness shows no change in the direction, which is broadly orthogonal to paleoflow, while decreasing in a downstream direction from ~1.05 to 0.7 m over a distance of ~750 m.

Bed B comprises several small ribbons which are located in the thickest parts of the amalgamated sandstone sheet. These ribbons at similar stratigraphic levels are connected by thin sandstone sheets and indicate that several channels were active either at the same time or close to each other and may have formed an anastomosed and/or distributary

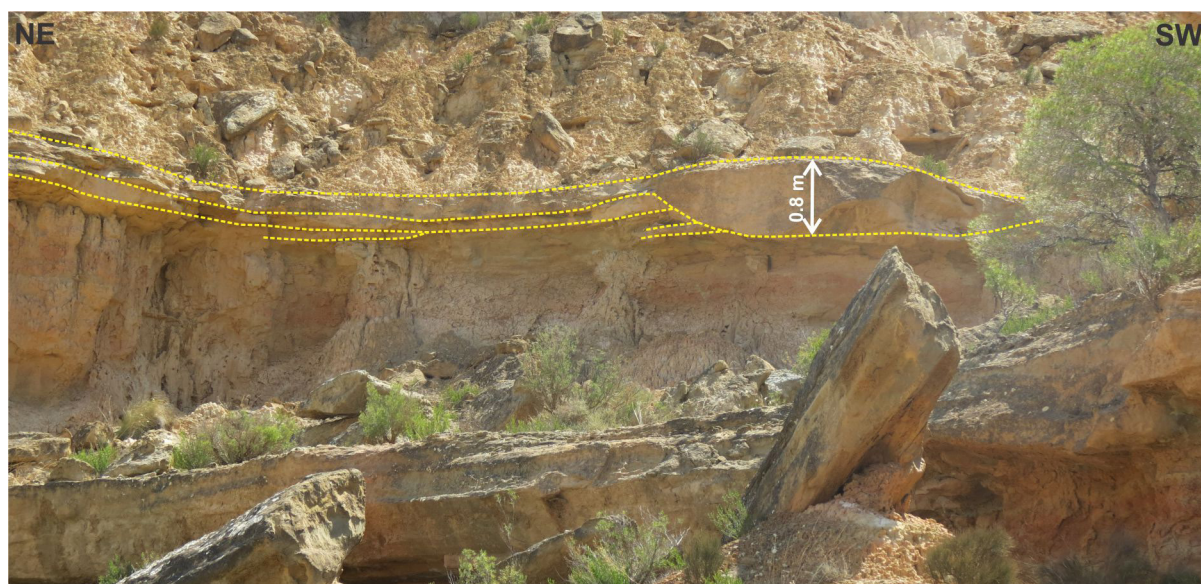


Fig. 9 - A minor ribbon sandstone (0.8 m thick at the central part, ~ 6 m wide) lying above a thin sandstone sheet (0.1 m thick) with an erosional contact. The ribbon sandstone is composed of structureless fine-grained sand and shows no variation in grain size. It constitutes the filling of a channel, cut through underlying older splay deposits, which was abandoned following local avulsion and then filled with sand due to high sediment supply at the distal part of the DFS.

pattern. These ribbons are structureless, no paleocurrent indicators were observed, however, paleocurrents measured from thin sheet sandstone in the whole bed B show a wide dispersion (130° - 340°) which strongly suggests, but does not prove, a distributary pattern. Their locations in the thickest parts of the amalgamated sandstone sheets also support this interpretation as splay deposits thin away from the proximal part of splay and thin sheet sandstones occur in the marginal parts. Convex-up beds comprising sandstone bedsets that onlap onto older convex-up sandstone deposits (Fig. 8) were observed in the thickest part of bed B. This lobe-like feature can be interpreted as resulting from new flow events depositing sediment rapidly and prograding (the deposits on the top part of the sandbody) over the older splay deposits (the lower sandstone unit).

The very fine to fine-grained thin sandstone sheets (0.05-2.0 m thick, laterally extensive up to several 100 m) interbedded with thick mudstones/siltstones (up to 9 m thick) observed in the study area are interpreted as splay deposits. This interpretation is supported by the characteristics of the deposits and includes the slightly convex-up upper surface of the ribbon sandstones (Fig. 9), lobe-like features (Fig. 8) and the downstream decreasing trends in thicknesses and grain size of sandstone units.

The distribution of facies and architectural elements that are described and interpreted above suggests that the studied section represents part of one or several splay complexes. If the splay deposits of the studied section correspond to crevasse splays fed by crevasse channels, all lateral to the main trunk river system, it would be expected that they would be present throughout the entire system potentially as precursors to each channel reoccupation. This is explained by the development of

a new single main channel through a former crevasse channel associated with a crevasse splay (Smith et al., 1989; Stouthamer, 2001; Slingerland and Smith, 2004; Jones and Hajek, 2007; Hajek and Edmond, 2014). However, splay complexes are present only in the distal part of the Huesca System, not in the proximal and medial parts (Hirst and Nichols, 1986; Hirst, 1991). In addition, the dominantly south-west paleocurrent directions in the studied section are consistent with the main channel system orientation (Hirst and Nichols, 1986; Hirst, 1991). These relationships support an interpretation of the studied section as a terminal splay complex rather than a crevasse splay complex lateral to a larger fluvial channel that was subject to repeated river avulsions. This is further supported by the absence of multistorey channel deposits in any of the studied sections or indeed throughout the adjacent area, indicating no relationship to a larger channel system. Further support is provided by the absence of associated levee deposits with the ribbon and sheet sandstones which infers that sheetfloods occurred during bank-full flow conditions and were relatively orthogonal to the confining channel.

4. DISCUSSION

The observed radial pattern of the Parapeti DFS is not formed by simultaneously active distributary channels as the Gash River and the Markanda River in the model of Kelly and Olsen (1993), but is the result of successive multiple random avulsions as in the model of Nichols and Fisher (2007). Both active and abandoned channels of the Parapeti River generally display downstream decreases in channel size, coupled with a radial pattern of channels away from the apex and a lack of lateral

channel confinement. These combined characteristics are consistent with DFS models (Kelly and Olsen, 1993; Nichols and Fisher, 2007; Weissmann et al., 2010) which predict a decrease in channel size, grain size of channel-fill facies and interconnectedness down-system. These down-system trends suggest a downstream decrease in energy, which is attributed to channel bifurcation, infiltration and evapotranspiration (Kelly and Olsen, 1993; Nichols and Fisher, 2007; Hartley et al., 2010; Weissmann et al., 2010; Davidson et al., 2013). The climate in the Parapeti DFS is semi-arid and characterised by a high evaporation to precipitation ratio, thus evaporation can help to reduce flow strength in the system. The sandy substrate underlying the Parapeti River have a relatively high permeability and contribute partly to the downstream decrease in flow discharge due to infiltration across this zone (Tooth, 1999; Donselaar et al., 2013).

Channel bifurcation is present in the distal part of the current Parapeti River and is not observed in the proximal or medial zones. A decrease in channel size toward the river termination such that the channel cannot accommodate discharge during peak flood events, leads to bifurcation and terminal splay formation. Through time, terminal splay deposits have built up, forming a low amplitude lobate sand-body on the floodplain. This is attributed to a reduction in energy of the floodwater as the flow expands away from the channel. As a result, floods deposit most of their sediment load near the channel mouth with sediment thicknesses decreasing away from the channel mouth. The sandstone lobe will be at a higher elevation relative to the adjacent areas. Consequently, it will promote local avulsion of the active channel at the distal part of the DFS. The progradation of the Parapeti River terminus is similar to that of the Gash River terminus (Abdullatif, 1989). However, there are examples where bifurcation of active channels occurs on a large scale, such as the Okavango system (Stanistreet and McCarthy, 1993) and the Taquari River (Assine, 2005; Buehler et al., 2011; Weissmann et al., 2011) which also show a decrease in channel size down-system, ultimately terminating in splays in the distal zone of the DFS.

Fluvial deposits from the Miocene age Huesca DFS show a down-system decrease in thickness of amalgamated channel sandstone bodies, decrease in sand percentage and overall system grain size, and increase in proportion of floodplain deposits relative to amalgamated channel facies associations (Hirst, 1991; Kulikova, 2013). The observations in this study are also consistent with the findings of other researchers (Hirst, 1991; Fisher et al., 2007; Kulikova, 2013). These combined features are share some similarities with the Parapeti DFS. These combined features also suggest a decrease in stream power down-system due to infiltration, evapotranspiration, channel bifurcation and deceleration of flow as the system radiates from the DFS apex (Nichols and Fisher, 2007; Hartley et al., 2010; Weissmann et al., 2010). The climate in the Ebro Basin during the Oligocene-Miocene is considered to have been temperate (Hamer et al., 2007), but net evaporation

within the basin is thought to have been greater than input from precipitation (Nichols and Hirst, 1998), such that evaporation would have been an additional control on downstream flow reduction. Amalgamated sandstone bodies in the proximal and medial parts of the Huesca DFS succession (Hirst, 1991) would have provided a substrate suitable for infiltration. By incorporating results from numerical studies of the Miocene Huesca DFS and with our observations at the distal part, a conceptual model for the Huesca DFS is proposed (Fig. 10a).

The Parapeti and Huesca fluvial systems both present distributive fluvial channel patterns of channel and floodplain deposits that radiate away from their apices located where the fluvial systems enter the sedimentary basin. The size of the Parapeti DFS (150 km radius, area >5800 km²) is more than twice that of the Huesca DFS (60 km radius, area ~3000 km²). Despite differences in size, the Miocene age Huesca DFS and the modern Parapeti DFS reveal many similarities.

The coarser-grained size, high amalgamated sandstones portion of the Huesca succession is comparable to the proximal zone of the Parapeti DFS (<50 km from the apex) where highly amalgamated sand-bodies are likely to be present due to frequent channel shifting back and forth across a relatively narrow area. This will result in erosion of older channel belt deposits and removal of finer grained material.

The medial parts of the Huesca and Parapeti DFS are also likely to be comparable with less amalgamated sand-body development due to increased lateral mobility of channel belts across a wider area of the DFS relative to the proximal zone concomitant with a decrease in grain size. Fine-grained deposits intercalated with discrete channel belt deposits are observed on satellite imagery. However, there is a difference between two DFSs in this zone. The Huesca DFS shows a decrease in channel-fill dimension downstream, while the channel-belt width of the Parapeti DFS in the medial part is larger than in the proximal part showing a decreasing trend only in the distal part. This may be attributed to the gentler gradient channel in the medial part than in the proximal part leading the river becomes wider and shallower in the medial part due to flow velocity decrease.

The portion of the Huesca DFS succession which is composed predominantly of floodplain facies association is comparable to the distal zone of the Parapeti DFS. Based on analysis of the remotely sensed data, several splays at the distal part of the Parapeti River have been recorded. The splay deposits have a wide range of spatial scales ~0.5-30 km² with the length ranging from several meters to 18 km. Similarly, the distal sector of the Miocene Huesca DFS is characterized by an abundance of sheet-like sandstones, amalgamated sandstone sheets and ribbon sandstones interpreted as splay deposits with a wide range of dimensions. As the splays formed and enlarged at the terminus of the Parapeti River during the investigated period, adjacent splays became amalgamated through a combination of compensational

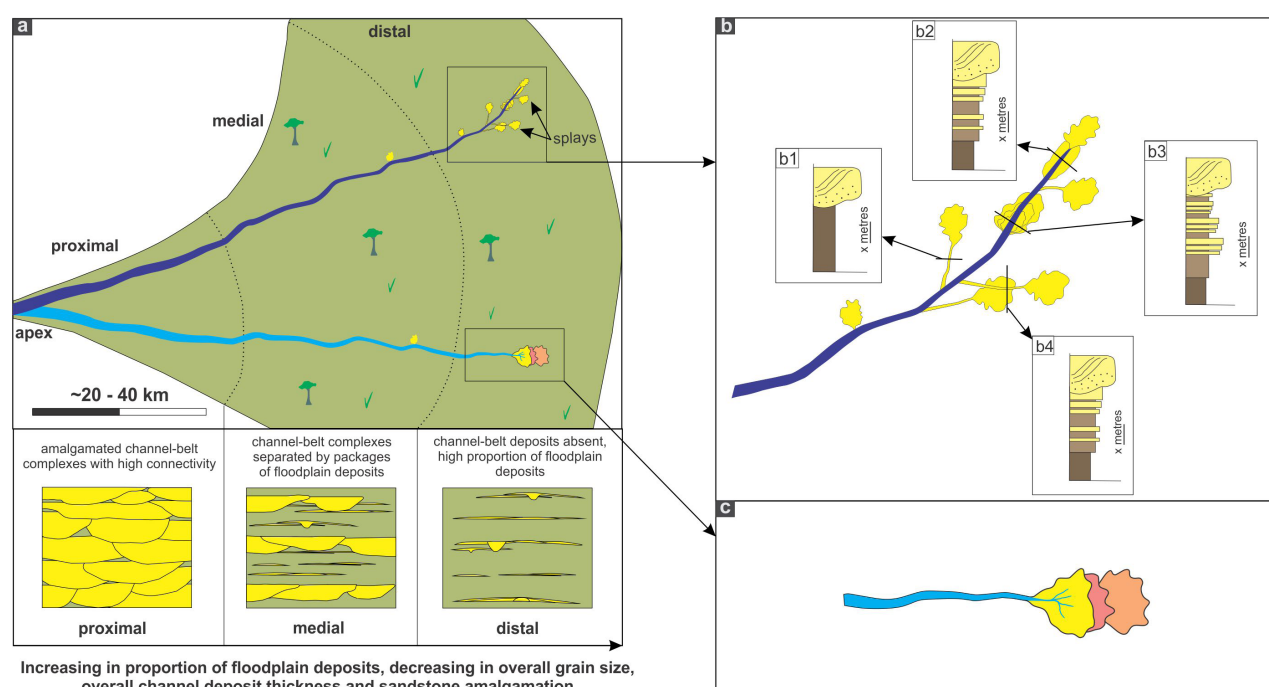


Fig. 10 - a) schematic diagram that summarizes the conceptual depositional models built for the Parapeti and Huesca DFSs; b) Examples of coarsening- and thickening-upward facies sequences occurring in the DFSs that are related to the avulsion, progradation and retrogradation processes of the system; the recognized features are very similar to the avulsion deposits described by Jones and Hajek, 2007.

stacking and local avulsion following a major flood event approximately every 20 years. Similarly, the multiple amalgamated sandstone sheets in the distal zone of the Huesca DFS suggest deposition from multiple flow events with relatively short repeat times as indicated by a lack of bioturbation or paleosol development.

The larger channel belt width and splay dimensions of the modern Parapeti DFS relative to the Huesca DFS is related to the variation in a combination of factors including fluvial system scale, discharge regime, sediment supply, surface gradient, bank cohesion and the density and type of floodplain vegetation. Both systems are characterised by pronounced seasonality and high evaporation to precipitation ratio, thus evaporation could have partly contributed to the flow power reduction downstream in both DFSs. Additionally, both studied systems have sandy substrates in the proximal and medial zones which have relatively high permeability, promoting infiltration across these zones. Paleoenvironmental reconstructions for the Huesca DFS by Hamer et al. (2007) suggested that the area was covered by low stature plants, shrubs, herbs, small open woodland trees and herbaceous vegetation which prevent significant erosion of floodplain deposits (Turner and Peterson, 2004). Semi-deciduous Chaco dry forest occupying the area along the Parapeti River (May, 2013) may contribute to the cohesiveness of the channel banks. It is likely that sediment supply and discharge play important roles in the difference between the dimension of the channel belts and splays of the Parapeti and Huesca DFSs.

It is observed that channel avulsion is a common

process on the distal zone of the Parapeti DFS, controlling sediment distribution through terminal splay formation. This can result in a complex relationship between sandstone bodies formed by lateral and terminal splays and the main channel. Channel avulsion has long been defined as the process responsible for the abrupt relocation of a channel to a lower gradient (Smith et al., 1989; Mohrig et al., 2000; Slingerland and Smith, 2004). A reduction in downstream gradient owing to base level rise and following increased sinuosity, or an increase in lateral gradient are suggested the causes of channel avulsion (Jones and Schumm, 2009). Of these potential causes, an increase in lateral gradient due to formation of terminal splay deposits resulting in increased elevation of the terminal lobe relative to the adjacent area is likely to be the major cause of avulsion in the distal part of the Parapeti River. Blockages in the channel due to increased sediment supply (Smith et al., 1989; McCarthy et al., 1992; Bridge, 2003) may lead to increased deposition within the channel, encouraging avulsion to occur.

Three main types of avulsion in modern rivers are recognised: (1) avulsion via progradation, following splay deposition; (2) avulsion via re-occupation/annexation, with reoccupation of abandoned channel or appropriation of existing channels; (3) avulsion through incision, caused by scouring of a new channel (Slingerland and Smith, 2004). Recent research suggests that avulsion by progradation and avulsion by incision are identifiable in the rock record (Smith et al., 1989; Kraus and Wells, 1999; Mohrig et al., 2000; Jones and Hajek, 2007). A coarsening- and thickening-upward sequence of proximal-overbank

(splays) deposits beneath a channel-belt was suggested to indicate avulsion via splay progradation (Kraus and Wells, 1999; Slingerland and Smith, 2004; Jones and Hajek, 2007; Hajek and Edmonds, 2014). Examples supporting this model are presented for the Eocene Willwood Formation, Bighorn Basin, Wyoming, USA (Kraus, 1999; Kraus and Wells, 1999), Holocene Rhine-Meuse Delta deposits (Stouthamer and Berendsen, 2000) and the Cumberland Marshes – Saskatchewan (Smith et al., 1989). In contrast, avulsion through incision is represented by channel-belt deposits directly overlying floodplain deposits (Jones and Hajek, 2007). Examples for this are the Wasatch Formation (Mohrig et al., 2000) and the Ferris Formation (Jones and Hajek, 2007).

One example of avulsion styles in the distal part of the Parapeti River formed where a new main channel cut through previous splay deposits. As such, the splay deposits beneath the channel-belt are unrelated to the avulsion, but if preserved in a vertical succession, are likely to appear similar to the stratigraphically transitional avulsion deposits defined by Jones and Hajek (2007) (Fig. 10b4) or the avulsion stratigraphy model outlined by Kraus and Wells (1999). Furthermore, the splay deposits beneath the channel-belt may not show an idealised coarsening- and thickening-upward profile. For example, it is likely that splay deposits formed through several episodes of unconfined flows with variable discharge and sediment concentrations, resulting in variable size and thicknesses of splay deposits. Thus, channel-belts may overlie or cut through multiple splays composed of vertically stacked intervals of relatively distal and/or proximal splay deposits of different sizes and thicknesses without the development of any preferred vertical stratigraphic succession (Fig. 10b3). In addition, other examples of avulsion on the Parapeti illustrated above occur where a new channel avulses onto the floodplain and does not incise and scour older splays, such that the stratigraphy would be similar to the stratigraphically abrupt example of Jones and Hajek (2007) (Fig. 10b1). Therefore, both succession styles proposed by Jones and Hajek (2007) will occur adjacent to and potentially interbedded with each other if the distal portion of the Parapeti DFS was to be preserved (Fig. 10).

Jones and Hajek (2007) suggested that one type of avulsion style tends to prevail within an individual fluvial system dependent on whether during flood events the fluvial system was prone to producing splays or overbank deposition without splay development. Crevasse splay prone fluvial systems produce the stratigraphically transitional succession whereas the more overbank flood sediment dominated systems produced the stratigraphically abrupt succession (Jones and Hajek, 2007). This was based on observations from the Willwood Formation which appears to be dominated by the stratigraphically transitional avulsion style, whereas the Ferris Formation is dominated by the stratigraphically abrupt avulsion stratigraphy (Jones and Hajek, 2007). Splay proneness of a fluvial system has been considered

to be a function of grain size distribution, channel bank cohesiveness, levee sizes, elevation differences between channel water level and adjacent floodplain and variable hydrographs (Jones and Hajek, 2007 and references therein). For instance, a fluvial system having levees with low topographic relief, high magnitude flooding events and highly cohesive banks (e.g., the Fitzroy River, northwest Australia – Taylor, 1999; the Ferris Formation – Jones and Hajek, 2007) would dominantly produce stratigraphically abrupt channels. In contrast, a dominantly sandy system having sandier levees (e.g. the Willwood Formation, Bighorn Basin, Wyoming, USA) with less cohesive banks would promote the formation of splays and thus formation of stratigraphically transitional avulsion successions. The Ferris Formation (Hanna Basin, Wyoming, USA) has a bimodal grain size distribution in which very fine-grained (silt and clay) material dominates overbank deposits (Jones and Hajek, 2007), lacking sufficient suspended sandy material to deposit splays. Such a grain size distribution will also favour the development of stratigraphically abrupt avulsion successions (Jones and Hajek, 2007).

The Parapeti River is a sandy system with the levees composed of coarse (sandy) sediments (Iriondo, 1993) and should produce a dominantly transitional avulsion succession through avulsion by splay progradation where a new trunk channel is gradually established over widespread crevasse splay progradation as suggested by Jones and Hajek (2007). However, abundant vegetation along the Parapeti River may make river banks more cohesive. In addition, high magnitude flood events in the system are supposed to favour abrupt avulsion (Jones and Hajek, 2007). In fact, the avulsions observed in the Parapeti River in the investigated time period are stratigraphically abrupt incision avulsions where the new channel incises into both floodplain and splay deposits, with splay deposits also being abundant in regions distal to the channel. Therefore, the Parapeti system could be termed a mixed avulsion style system that is intermediate between the abrupt and transitional styles of Jones and Hajek (2007). Consequently, the avulsion style cannot simply be related to the “proneness” of the fluvial system to form splay deposits as proposed by Jones and Hajek (2007).

In addition, the presence of stratigraphically transitional or stratigraphically abrupt avulsion successions, which can both be formed by local avulsions in the Parapeti DFS, are unlikely to infer the relative avulsion distance to the parent channel as suggested by Jones and Hajek (2007). These authors suggested that transitional and abrupt types of avulsion succession may indicate local and regional avulsions, respectively. For example, an avulsed channel is more likely to occur above sandy overbank deposits if it is close to the parent channel, while potentially overlying finer-grained floodplain deposits where it is further from the parent channel (Jones and Hajek, 2007).

Furthermore, the stratigraphic succession of the Parapeti DFS where the terminal splay gradually

progressed through preceding splays and the terminus propagated further downstream following successive discharge events would result in a succession similar to the stratigraphically transitional avulsion succession proposed by Jones and Hajek (2007) (Fig. 10b2). However, no avulsion has taken place in this scenario, rather the system has simply prograded downstream (Fig. 10b2).

Coarsening- and thickening-upward sequence of proximal-overbank (splays) deposits beneath a channel-belt as well as channel-belt deposits juxtaposed directly atop fine-grained floodplain deposits in the Miocene Huesca DFS were reported by Kulikova (2013). These heterolithic overbank deposits of the Huesca DFS succession exhibit both what appear to be transitional and abrupt avulsion successions. Additionally, Kulikova (2013) recognised vertically stacked packages of multiple splay deposits beneath the channel sandstones in the relatively proximal and medial parts of the Huesca DFS. These findings suggest that the avulsion processes on the Huesca DFS may be similar to that of the Parapeti DFS.

5. CONCLUSIONS

The conceptual depositional models for the Parapeti and Huesca DFSs have been established, representing a radial pattern of channel distribution away from the apex with a general decrease in channel size downstream, ultimately terminating in splays in the distal zones. Down-system trends include an increase in proportion of overbank deposits coupled with an overall decrease in channel size, mean grain size, percentage of sand and interconnectedness of sandstone bodies. These changes are interpreted to be controlled mainly by a reduction in flow strength as flows expand laterally, downstream of basin margin valleys as well as infiltration, evaporation and channel bifurcation within the basin.

Despite differences in size, the Parapeti and Huesca DFSs share many similarities in the downstream trends as illustrated in the conceptual models. Channel progradation and avulsion are interpreted to be the main processes that control facies formation and distribution within these DFSs.

It is likely that both succession styles proposed by Jones and Hajek (2007) will occur adjacent to and potentially interbedded with each other if the Parapeti DFS was to be preserved and do not have the same causal mechanisms inferred by Jones and Hajek (2007). In addition, the splay deposits beneath the channel-belt may not show an idealised coarsening-and thickening-upward profile. Furthermore, the avulsion styles proposed by Jones and Hajek (2007) can also be produced simply through progradation of the distal portion of a terminal splay that is unrelated to avulsion.

The Parapeti system could be termed a mixed avulsion style transitional between the abrupt and transitional styles of Jones and Hajek (2007), however, the avulsion style cannot simply be related to the “proneness” of the fluvial system to form splay deposits as suggested by

Jones and Hajek (2007).

Examples of stratigraphic successions that show characteristics of transitional and abrupt avulsion deposits, and examples of vertically stacked packages of multiple splay deposits occurring beneath channel sandstones in the Miocene Huesca DFS succession reported by Kulikova (2013), suggest that avulsion processes on the Huesca DFS are similar to those on the Parapeti DFS.

ACKNOWLEDGEMENTS - Financial support for this study was provided by Vietnamese Government Scholarship and Vietnam Oil and Gas Group. I also wish to thank to the sponsors of the Fluvial Systems Research Group (FSRG): BG, BP, Chevron, ConocoPhillips, and Total, for covering field and conference expenses. I also very grateful to reviewers for their constructive and helpful comment that helped to improve the manuscript.

REFERENCES

- Abdullatif O.M., 1989. Channel-fill and sheet-flood facies sequences in the ephemeral terminal River Gash, Kassala, Sudan. *Sedimentary Geology* 63, 171-184.
- Allen J.R.L., 1964. Studies in fluvial sedimentation: six cyclothems from the Lower Red Sandstone, Anglo-Welsh Basin. *Sedimentology* 3, 163-198.
- Anderson D.S., 2005. Architecture of crevasse splay and point-bar bodies of the nonmarine Iles Formation north of Rangely, Colorado: Implications for reservoir description. *The Mountain Geologist* 42, 109-122.
- Assine M.L., 2005. River avulsions on the Taquari megafan, Pantanal wetland, Brazil. *Geomorphology* 70, 357-371.
- Ayers Jr.W.B., 2002. Coalbed gas systems, resources, and production and a review of contrasting cases from the San Juan and Powder River basins. *American Association of Petroleum Geologists Bulletin* 86, 1853-1890.
- Bridge J.S., 2003. *River and Floodplain: Forms, Processes, and Sedimentary Record*. Oxford, Blackwells.
- Bryant R.G., 1996. Validated linear mixture modelling of Landsat TM data for mapping evaporite minerals on a playa surface: methods and applications. *International Journal of Remote Sensing* 17, 315-330.
- Buehler H.A., Weissmann G.S., Scuderi L.A., Hartley A.J., 2011. Spatial and temporal evolution of an avulsion on the Taquari river distributive fluvial system from satellite image analysis. *Journal of Sedimentary Research* 81, 630-640.
- Choukroune P., ECORS-Pyrenees Team, 1989. The ECORS Pyrenean deep seismic profile reflection data and the overall structure of an orogenic belt. *Tectonics* 8, 23-39.
- Davidson S.K., Hartley A.J., Weissmann G.S., Nichols G.J., Scuderi L.A., 2013. Geomorphic elements on modern distributive fluvial systems. *Geomorphology* 180-181, 82-95.
- Donselaar M.E., Overeem I., Reichwein J.H.C., Visser C.A., 2011. Mapping of fluvial fairways in the Ten Boer Member, southern Permian Basin. In: Grottsch J., Gaupp R. (Eds.), *The Permian Rotliegendes in the Netherlands*. SEPM Society for Sedimentary Geology, Special Publication 98, 105-118.
- Donselaar M.E., Cuevas Gozalo M.C., Moyano S., 2013. Avulsion processes at the terminus of low-gradient semi-

- arid fluvial systems: Lessons from the Río Colorado, Altiplano endorheic basin, Bolivia. *Sedimentary Geology* 283, 1-14.
- Fisher J.A., Nichols G.J., Waltham D.A., 2007. Unconfined flow deposits in distal sectors of fluvial distributary systems: Examples from the Miocene Luna and Huesca Systems, northern Spain. *Sedimentary Geology* 195, 55-73.
- Fisher J.A., Nichols G.J., 2013. Interpreting the stratigraphic architecture of fluvial systems in internally drained basins. *Journal of the Geological Society* 170, 57-65.
- Flores R.M., 1985. Coal deposits in Cretaceous and Tertiary fluvial systems of the Rocky Mountain Region. In: Flores R.M., Ethridge F.G., Miall A.D., Galloway W.E., Fouch T.D. (Eds.), *Recognition of Fluvial Depositional Systems and Their Resource Potential*. SEPM Society for Sedimentary Geology, Short Course 19, 167-216.
- Friend P.F., 1978. Distinctive features of some ancient river systems. In: Miall A.D. (Ed.), *Fluvial Sedimentology*. Canadian Society of Petroleum Geologists, Memoir 5, 531-542.
- Friend P.F., Slater M.W., Williams R.C., 1979. Vertical and lateral building of river sandstone bodies, Ebro Basin, Spain. *Journal of the Geological Society of London* 136, 39-46.
- Friend P.F., Hirst J.P.P., Nichols G.J., 1986. Sandstone-body structure and river process in the Ebro Basin of Aragon, Spain. *Cuadernos de Geología Ibérica* 10, 9-30.
- Hajek E., Edmonds D., 2014. Is river avulsion style controlled by floodplain morphodynamics? *Geology* 42, 199-202.
- Hamer J.M.M., Sheldon N.D., Nichols G.J., Collinson M.E., 2007. Late Oligocene-Early Miocene paleosols of distal fluvial systems, Ebro Basin, Spain. *Palaeogeography, Palaeoclimatology, Palaeoecology* 247, 220-235.
- Hartley A.J., Weissmann G.S., Nichols G.J., Warwick G.L., 2010. Large distributive fluvial systems: characteristics, distribution, and controls on development. *Journal of Sedimentary Research* 80, 167-183.
- Hirst J.P.P., 1991. Variations in alluvial architecture across the Oligocene-Miocene Huesca fluvial system, Ebro Basin, Spain. In: Miall A.D., Tyler N. (Eds.), *The Three-Dimensional Facies Architecture of Terrigenous Clastic Sediments and Its Implications for Hydrocarbon Discovery and Recovery*. SEPM Society for Sedimentary Geology, Concepts in Sedimentology and Paleontology 3, 111-121.
- Hirst J.P.P., Nichols G., 1986. Thrust tectonic controls on Miocene alluvial distribution patterns, southern Pyrenees. In: Allen P.A., Homewood P. (Eds.), *Foreland Basins*. International Association of Sedimentologists, Special Publication 8, 247-258.
- Horton B.K., De Celles P.G., 2001. Modern and ancient fluvial megafans in the foreland basin system of the central Andes, southern Bolivia: implications for drainage network evolution in fold-thrust belts. *Basin Research* 13, 43-63.
- Iriondo M., 1993. Geomorphology and late Quaternary of the Chaco (South America). *Geomorphology* 7, 289-303.
- Jones H.L., Hajek E.A., 2007. Characterizing avulsion stratigraphy in ancient alluvial deposits. *Sedimentary Geology* 202, 124-137.
- Jones L.S., Schumm S.A., 2009. Causes of avulsion: An overview. In: Smith N.D., Rogers J. (Eds.), *Fluvial Sedimentology VI*. International Association of Sedimentologists, Special Publication 28, 171-178.
- Jordan T.E., 1995. Retroarc foreland and related basins. In: Busby C.J., Ingersoll R.V. (Eds.), *Tectonics of Sedimentary Basins*. Cambridge, Massachusetts, Blackwell Science, pp. 331-362.
- Kelly S.B., Olsen H., 1993. Terminal fans - a review with references to Devonian examples. *Sedimentary Geology* 85, 339-374.
- Kraus M.J., 1999. Paleosols in clastic sedimentary rocks: their geologic applications. *Earth-Science Reviews* 47, 41-70.
- Kraus M.J., Wells T.M., 1999. Recognizing avulsion deposits in the ancient stratigraphical record. In: Smith N.D., Rogers J. (Eds.), *Fluvial Sedimentology VI*. International Association of Sedimentologists, Special Publication 28, 251-268.
- Kulikova A., 2013. Architecture of distributive fluvial system deposits: quantitative characterization and implications to reservoir modelling. PhD. Thesis, Royal Holloway, University of London.
- May J.H., 2013. Dunes and dunefields in the Bolivian Chaco as potential records of environmental change. *Aeolian Research* 10, 89-102.
- McCarthy T.S., Ellery W.N., Stanistreet I.G., 1992. Avulsion mechanisms on the Okavango fan, Botswana: the control of a fluvial system by vegetation. *Sedimentology* 39, 779-795.
- Miall A.D., 1996. *The Geology of Fluvial Deposits: Sedimentary facies, basin analysis, and petroleum geology*. Springer-Verlag, New York, pp. 582.
- Mohrig D., Heller P.L., Paola C., Lyons W.J., 2000. Interpreting avulsion process from ancient alluvial sequences: Guadalupe-Matarranya system (northern Spain) and Wasatch Formation (western Colorado). *Geological Society of America Bulletin* 112, 1787-1803.
- Munoz J.A., 1992. Evolution of a continental collision belt: ECORSPyrenees crustal balanced cross-section. In: McClay K.R. (Ed.), *Thrust Tectonics*. Chapman and Hall, London, pp. 235-246.
- Nichols G.J., Fisher J.A., 2007. Processes, facies and architecture of fluvial distributary system deposits. *Sedimentary Geology* 195, 75-90.
- Nichols G.J., Hirst J.P.P., 1998. Alluvial fans and fluvial distributary systems, Oligo-Miocene, northern Spain: contrasting processes and products. *Journal of Sedimentary Research* 68, 879-889.
- Pashin J.C., 1998. Stratigraphy and structure of coalbed methane reservoirs in the United States: an overview. *International Journal of Coal Geology* 35, 209-240.
- Quarby N.A., Townshend J.R.G., Millington A.C., White K., Reading A.I., 1989. Monitoring sediment transport systems in a semiarid area using thematic mapper data. *Remote Sensing of Environment* 28, 305-315.
- Rosenfeld C.L., 1984. Remote sensing techniques for geomorphologists. In: Costa J.E., Fleisher P.J. (Eds.), *Developments and Applications of Geomorphology*. Springer, pp. 1-37.
- Scott S., Anderson B., Crosdale P., Dingwall J., Leblang G., 2007. Coal petrology and coal seam gas contents of the Walloon

- Subgroup-Surat Basin, Queensland, Australia. *International Journal of Coal Geology* 70, 209-222.
- Shanley K.W., Cluff R.M., Robinson J.W., 2004. Factors controlling prolific gas production from low-permeability sandstone reservoirs: Implications for resource assessment, prospect development, and risk analysis. *American Association of Petroleum Geologists Bulletin* 88, 1083-1121.
- Slingerland R., Smith N.D., 2004. River avulsions and their deposits. *Annual Review of Earth and Planetary Sciences* 32, 257-285.
- Smith N.D., Cross T.A., Dufficy J.P., Clough S.R., 1989. Anatomy of an avulsion. *Sedimentology* 36, 1-23.
- Stanistreet I.G., McCarthy T.S., 1993. The Okavango fan and the classification of subaerial fan systems. *Sedimentary Geology* 85, 115-133.
- Stouthamer E., 2001. Sedimentary products of avulsions in the Holocene Rhine-Meuse delta, The Netherlands. *Sedimentary Geology* 145, 73-92.
- Stouthamer E., Berendsen H.J.A., 2000. Factors controlling the Holocene avulsion history of the Rhine-Meuse Delta, The Netherlands. *Journal Sedimentary Research* 70A, 1051-1064.
- Taylor C.F.H., 1999. The role of overbank flow in governing the form of an anabranching river: the Fitzroy River, northwestern Australia. In: Smith N.D., Rogers J. (Eds.), *Fluvial Sedimentology VI*. International Association of Sedimentologists, Special Publication 28, 77-92.
- Teixell A., 1996. The Ansó transect of the southern Pyrenees: basement and cover geometries. *Journal of the Geological Society* 153, 301-310.
- Tooth S., 1999. Downstream changes in floodplain character on the northern Plains of arid central Australia. In: Smith N.D., Rogers J. (Eds.), *Fluvial Sedimentology VI*. International Association of Sedimentologists, Special Publication 28, 93-112.
- Turner C.E., Peterson F., 2004. Reconstruction of the Upper Jurassic Morrison Formation extinct ecosystem - a synthesis. *Sedimentary Geology* 167, 309-355.
- Uba C.E., Heubeck C., Hulka C., 2006. Evolution of the late Cenozoic Chaco foreland basin, Southern Bolivia. *Basin Research* 18, 145-170.
- Vergés J., Fernandez M., Martinez A., 2002. The Pyrenean orogen: pre-, syn- and post-collisional evolution. In: Rosenbaum G., Lister G.S. (Eds.), *Reconstruction of the Evolution of the Alpine-Himalayan Orogen*. *Virtual Explorer* 8, 55-74.
- Verstappen H.T., 1977. *Remote Sensing in Geomorphology*. Elsevier, Amsterdam, pp. 214.
- Weissmann G.S., Hartley A.J., Nichols G.J., Scuderi L.A., Olsen M., Buehler H., Banteah R., 2010. Fluvial form in modern continental sedimentary basins: Distributive fluvial systems. *Geology* 38, 39-42.
- Weissmann G.S., Hartley A.J., Nichols G.J., Scuderi L.A., Olsen M., Buehler H., Massengill L.C., 2011. Alluvial facies distributions in continental sedimentary basins - distributive fluvial systems. In: Davidson S.K., Leleu S., North C.P. (Eds.), *From River to Rock Record*. SEPM Society for Sedimentary Geology, Special Publication 97, 327-355.

